THE ASTROPHYSICAL JOURNAL SUPPLEMENT SERIES, 53:73–92, 1983 September

THE QUADRUPOLE OSCILLATIONS OF NEUTRON STARS[1]

LEE LINDBLOM
Institute of Theoretical Physics, Department of Physics, Stanford University
AND
STEVEN L. DETWEILER
Department of Physics, Yale University
Received 1982 October 4; accepted 1983 January 31

ABSTRACT

We investigate here the influence of the equation of state of matter (in the nuclear density regime) on the dynamical behavior of neutron stars. The properties of the quadrupole (f mode) oscillations of neutron stars constructed from 13 equations of state are presented. An efficient algorithm for computing the complex eigenfrequencies of the nonradial (p and f mode) oscillations of neutron stars is presented. The results of our computations are compared to relevant astrophysical observations.

Subject headings: dense matter — equation of state — stars: neutron — stars: pulsation

I. INTRODUCTION

Neutron stars provide a unique natural laboratory; strong gravitational fields and matter having supernuclear densities are balanced in objects of macroscopic dimensions. Since the macroscopic equilibrium parameters of neutron stars (masses, radii, moments of inertia, etc.) depend sensitively on the properties of matter at supernuclear densities (see Arnett and Bowers 1977), the observation of these parameters offers a unique opportunity to study matter at high densities. An even more sensitive test of the interior structure of a neutron star could be obtained by studying its dynamical behavior, viz., the oscillations of the star resulting from small nonequilibrium disturbances.

A number of observations have been made in recent years which are believed to be associated with perturbed neutron stars. These observations are presently of two classes. The first class of observations comprises γ-ray and X-ray burst phenomena. These events are clearly explosive in nature and have been associated with neutron stars by many authors (see, e.g., Ramaty and Lingenfelter 1981; Oda 1981). These explosive events probably perturb the associated neutron star, and the resulting dynamical behavior may eventually be deduced from such observations. The second class of observations come from pulsar timing measurements. Pulsars are generally believed to be rotating neutron stars. Observations of quasi-periodic subpulses have been identified with oscillations of the underlying neutron star by several authors (see, e.g., Boriakoff 1976; Van Horn 1980).

[1]This research was supported by National Science Foundation grants PHY81-18387 to Stanford University and PHY81-16482 to Yale University.

With this growing list of observational data which appears to be relevant to the study of oscillating neutron stars, we felt that it was appropriate at this time to prepare a careful survey of the effects of the structure of high density matter on the observables of oscillating neutron stars. To accomplish this we have computed numerical frequencies and eigenfunctions for a large number of neutron star models using 13 equations of state in the supernuclear density regime. We have chosen to use essentially the same set of equations of state and the same stellar models as those used by Arnett and Bowers (1977) in their extensive survey of the equilibrium parameters of neutron stars. In the present work we consider the lowest frequency quadrupole mode (the f mode), while in an accompanying paper Glass and Lindblom (1982) investigate the fundamental radial oscillation modes.

Thorne and co-workers were the first to consider the nonradial oscillations of a neutron star in a fully general relativistic context (Thorne and Campolattaro 1967; Price and Thorne 1969; Thorne 1969*a*, *b*; Campolattaro and Thorne 1970; Ipser and Thorne 1973). In these papers the formalism needed to describe the oscillation of a neutron star is derived. Thorne (1969*a*) integrated the resulting equations to determine numerical frequencies for the quadrupole modes of a very small number of neutron star models. Thorne's numerical techniques did not allow him to accurately determine the imaginary part of the oscillation frequency (the part caused by the damping of these modes by the emission of gravitational radiation). An alternative approach for the computation of the oscillation frequencies of neutron stars was developed by Detweiler and Ipser (1973). They found a variational principle which was used by Detweiler (1975)

to compute approximate oscillation frequencies for a more extensive set of neutron star models than those considered by Thorne. Detweiler's computations also had difficulty determining the imaginary part of the oscillation frequencies, due primarily to the smallness of the imaginary part relative to the real part (high Q) of these frequencies.

The present paper is an extension of the research outlined above. It was our aim to compute accurate oscillation frequencies (both real and imaginary parts) for a far wider range of neutron star models than had been considered previously by Thorne (1969*a*) and Detweiler (1975). We integrated the perturbation equations directly in a manner similar to Thorne (1969*a*). We modified Thorne's algorithm, however, in order to more efficiently compute the oscillation frequencies and to more accurately determine the imaginary parts of the frequencies. The details of our algorithm are discussed at length in the Appendices.

In § II of this paper we describe the equations of state which have been used by us to construct the stellar models whose oscillation frequencies are determined. In § III the graphical and tabulated results of our computations are presented and discussed. In the final section, § IV, our results are compared to the existing astrophysical observations (in particular, the 1979 March 5 γ-ray event).

II. THE EQUATIONS OF STATE

The aim of the present work is to survey the influence of the equation of state in the nuclear density regime on the properties of the oscillations of neutron stars. An extensive survey of the influence of the equation of state on the equilibrium properties of neutron stars was made by Arnett and Bowers (1977). We decided to extend their survey by computing the oscillation properties of the neutron star models whose equilibrium parameters they have cataloged. We have chosen, therefore, to use essentially the same set of equations of state used by them.

Table 1 lists the 13 equation of state models which we used in our computations. The reference given for each model generally refers to the nuclear density portion of that equation of state. For lower densities (except model H) combinations of the Feynman-Metropolis-Teller, the Baym-Pethick-Sutherland, and the Baym-Bethe-Pethick (see Baym, Pethick, and Sutherland 1971) equations of state are used. Our models are identical to those used by Arnett and Bowers (1977) except for models H and N. Our model H uses the Harrison-Wheeler equation of state, which differs at low densities from the noninteracting neutron Fermi gas model which was model H of Arnett and Bowers. We use the Harrison-Wheeler equation of state so that our oscillation frequencies may be compared to earlier work. Our model N is a more recent generalization of Walecka's (1974) relativistic mean field equation of state, which was model N of Arnett and Bowers. The model used by us is Serot's (1979) pure neutron equation of state.

Tabulated values for the equations of state used can generally be found in the references cited in Table 1. A convenient collection of many of them (models A–G and I) can also be found in Arnett and Bowers (1974). Numerical values for equation of state N were kindly provided by B. Serot and are reproduced here as Table 2. The actual values of the density and pressure needed for the calculation were obtained from these tables by logarithmic interpolation as described, for example, by Arnett and Bowers (1977).

The adiabatic index γ needed in the pulsation equation was computed by differentiating the equation of state according to the formula $\gamma = (\rho + p)p^{-1}dp/d\rho$. We computed γ for each value in the equation of state table by a simple difference formula; intermediate val-

TABLE 1

EQUATIONS OF STATE

Model	Reference	Density Range ($g\ cm^{-3}$)
A	Pandharipandi 1971 (neutron)	$\geq 7.004\times10^{14}$
B	Pandharipandi 1971 (hyperonic; model C)	$\geq 6.968\times10^{14}$
C	Bethe and Johnson 1974 (model I)	$\geq 1.706\times10^{14}$
D	Bethe and Johnson 1974 (model V)	$\geq 1.700\times10^{14}$
E	Moszkowski 1974	$\geq 2.200\times10^{14}$
F	Arponen 1972	$\geq 3.103\times10^{11}$
		$\leq 1.328\times10^{15}$
G	Canuto and Chitre 1974	$\geq 2.374\times10^{15}$
H	Hartle and Thorne 1968 (Harrison-Wheeler)	all
I	Cohen *et al.* 1970	$\geq 1.010\times10^{14}$
L	Pandharipande, Pines, and Smith 1976 (mean field)	$\geq 1.000\times10^{11}$
M	Pandharipande, Pines, and Smith 1976 (tensor)	$\geq 1.000\times10^{11}$
N	Serot 1979	$\geq 1.926\times10^{14}$
O	Bowers, Gleeson, and Pedigo 1975	$\geq 2.730\times10^{14}$

TABLE 2

THE SEROT EQUATION OF STATE

k_F (fm^{-1})	ρ (g cm^{-3})	p (dyne cm^{-2})
0.5	7.083×10^{12}	7.181×10^{30}
0.8	2.907×10^{13}	4.194×10^{31}
1.0	5.684×10^{13}	8.677×10^{31}
1.2	9.832×10^{13}	2.045×10^{32}
1.4	1.564×10^{14}	7.503×10^{32}
1.5	1.926×10^{14}	1.556×10^{33}
1.6	2.343×10^{14}	3.207×10^{33}
1.8	3.367×10^{14}	1.245×10^{34}
2.0	4.715×10^{14}	4.071×10^{34}
2.5	1.059×10^{15}	3.287×10^{35}
3.0	2.357×10^{15}	1.212×10^{36}
3.5	5.047×10^{15}	3.226×10^{36}
4.0	1.109×10^{16}	7.262×10^{36}
5.0	3.490×10^{16}	2.747×10^{37}

ues were found by interpolation. The adiabatic index computed in this way is appropriate only in the low frequency limit: when the oscillation periods are much longer than the reaction times needed to return the fluid to equilibrium (see, e.g., Meltzer and Thorne 1966). In practice there is little difference between the "equilibrium" γ used here and the "dynamical" γ for densities about $\sim 10^{13}$ g cm^{-3}. Since the majority of the matter in a typical (1 $M_\odot$) neutron star is at densities above this, little effect on the pulsation frequencies actually occurs because of this simplification.

The joining of the nuclear density equation of state, with the low density equation of state from Baym, Pethick, and Sutherland (1971) was done at a density chosen to make the result as continuous and smooth as possible. The density range used for each of the nuclear density equations of state is listed in Table 1. There are three anomalous cases. In model F, the Arponen (1972) equation of state does not extend beyond the nuclear density range. The higher density regime of model F (2.399×10^{15} g cm^{-3} and above) is taken to be the Pandharipandi (1971) hyperonic equation of state from our model B. In model G, the Canuto and Chitre (1974) solid neutron equation of state is applicable only at the highest densities. In the intermediate range between the low density equation of state and this high density region (between 6.968×10^{14} and 1.854×10^{15} g cm^{-3}) the Pandharipandi (1971) hyperonic model is again used. Finally, model H, the Harrison-Wheeler equation of state, is used for the complete range of densities.

III. THE RESULTS

We have computed the frequencies of the lowest quadrupole mode of oscillation for neutron stars constructed from the 13 equations of state models described in § II. The algorithm used to perform these computations is similar in principle to that developed by Thorne and Campolattaro (1967) and Thorne (1969*a*). We have made some modifications, however, to make the computations more efficient and to improve the accuracy of the imaginary parts of the frequencies. Our algorithm is described in detail in Appendix A.

The results of our computations are summarized in Figures 1–8 and Tables 3–15. Our tables contain four parameters which describe the properties of the equilibrium stellar model: ρ_c the central density, R the radius of the star, M the gravitational mass, and z the surface redshift of the star. There are in addition five parameters which describe the properties of the quadrupole ($l = 2$) mode having no radial nodes: T the oscillation period, τ the damping time of the mode, E the energy contained in the oscillations, and two parameters d_r and d_θ which describe the average radial and angular motion of the fluid at the surface of the star.

The equilibrium properties of these stellar models are discussed at length by Arnett and Bowers (1977). A great deal of additional information such as moments of inertia, binding energies, etc., can be found for these models from their work. We have chosen to tabulate here only the four parameters ρ_c, R, M, and z. The central density ρ_c is tabulated in units of 10^{15} g cm^{-3}. This parameter is the central boundary condition which we fix for our numerical integration of the equilibrium structure equations (A3)–(A5). The total radius of the

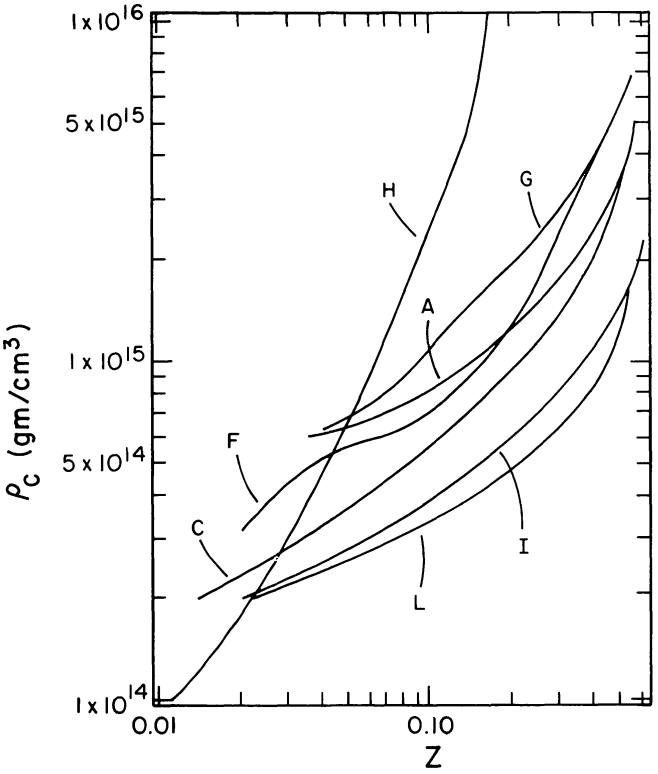

FIG. 1.—The surface redshift z is illustrated as a function of central density ρ_c for neutron stars constructed from equations of state A, C, F–L.

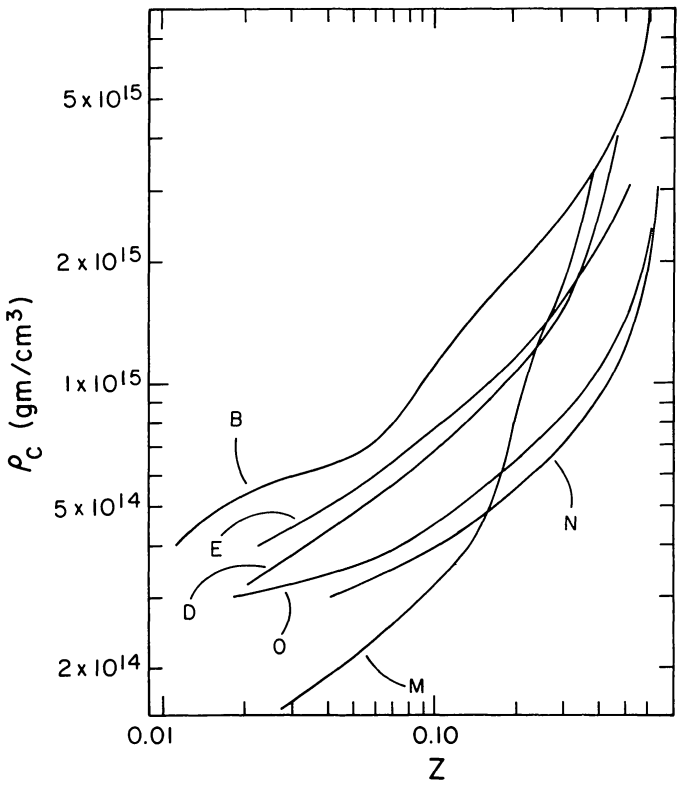

FIG. 2.—The surface redshift z is illustrated as a function of central density ρ_c for neutron stars constructed from equations of state B, D, E, M–O.

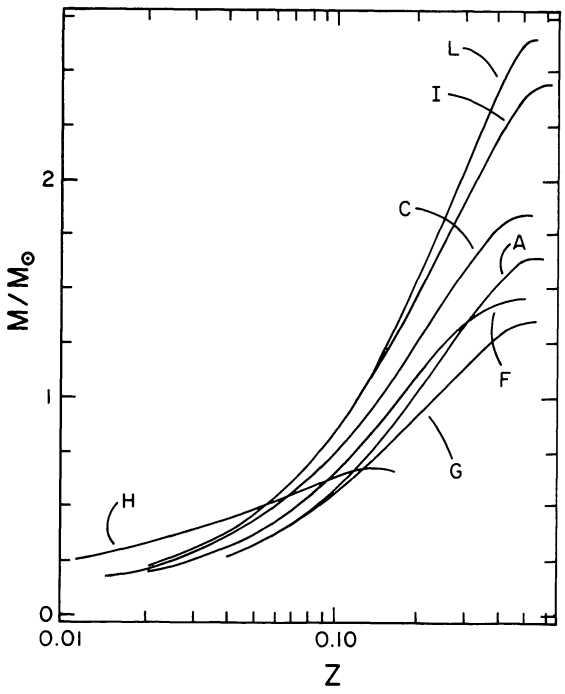

FIG. 3.—The total gravitational mass M is illustrated as a function of surface redshift z for neutron stars constructed from equations of state A, C, F–L.

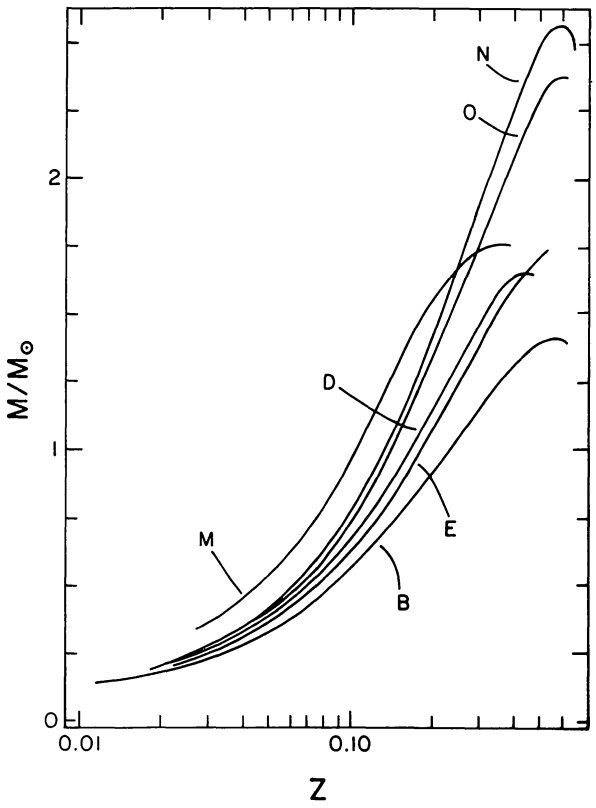

FIG. 4.—The total gravitational mass M is illustrated as a function of surface redshift z for neutron stars constructed from equations of state B, D, E, M–O.

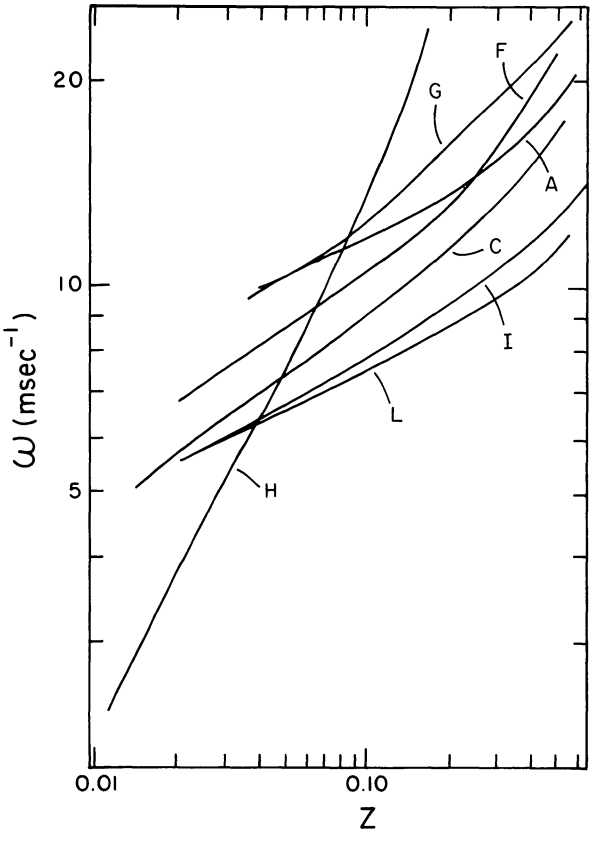

FIG. 5.—The oscillation frequency ω for the fundamental quadrupole mode is illustrated as a function of surface redshift z for neutron stars constructed from equations of state A, C, F–L.

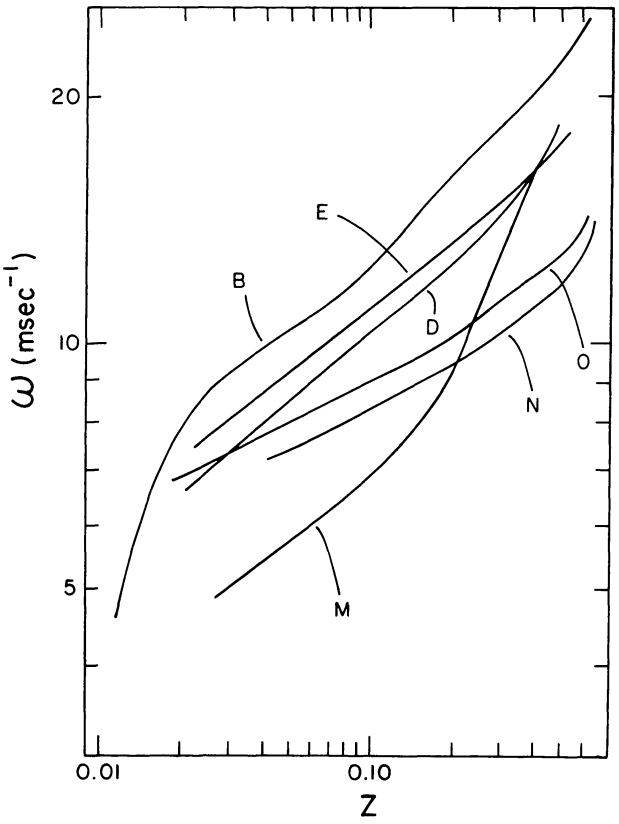

FIG. 6.—The oscillation frequency ω for the fundamental quadrupole mode is illustrated as a function of surface redshift z for neutron stars constructed from equations of state B, D, E, M–O.

stellar model R is tabulated in units of kilometers. We determine R from the condition that the pressure of our analytic polytropic "atmosphere" has a zero at R (see eqs. [A7]–[A8]). This total radius is probably our most poorly determined parameter; however, our values agree with those in Arnett and Bowers (1977) to within a few parts in 10^4. The total mass of the star M is tabulated in units of the mass of our Sun. This total mass is the value of the function $M(r)$ (see eq. [A2]) evaluated at the surface of the star $M = M(\mathrm{R})$. The parameter z corresponds to the redshift that a radially propagating photon would experience while traveling from the surface of the star to infinity. The parameter z is related to M and R by the simple equation:

$$z = (1 - 2M/R)^{-1/2} - 1. \qquad (1)$$

The redshift has been tabulated separately here because it is one parameter which may be observed directly. Emission lines in the 400–460 keV range have been observed in a number of γ-ray burst events (see, e.g., Mazets *et al.* 1981). These have been interpreted as the redshifted 511 keV $e^+ - e^-$ annihilation line. Assuming these events take place near the surface of a neutron star, one arrives at a direct determination of z. Figures 1 and 2 depict the relationship between the redshift and the central density, while Figures 3 and 4 depict the relationship between the redshift and the mass for the equilibrium models considered here.

When studying neutron star models with a fixed equation of state it is traditional to parameterize the equilibrium configurations by either the central density or the total mass. However, neither of these parameters seems appropriate for comparing models constructed from different equations of state. For example, a central density of 6×10^{14} g cm^{-3} corresponds to a very low mass and nonrelativistic model for equation of state A, $M = 0.26\ M_\odot$ and $z = 0.036$, but the same central density for equation of state L gives $M = 1.959\ M_\odot$ and $z = 0.275$. These are quite dissimilar neutron star models. Similarly the maximum stable mass varies from 1.4 to 2.6 $M_\odot$ for different equations of state. We find that stellar models having the same redshift parameter, z, are more directly comparable from one equation of state to another. From its definition, z gives a direct estimate of the importance of relativistic effects for a given model. Also, the neutron star families constructed from the

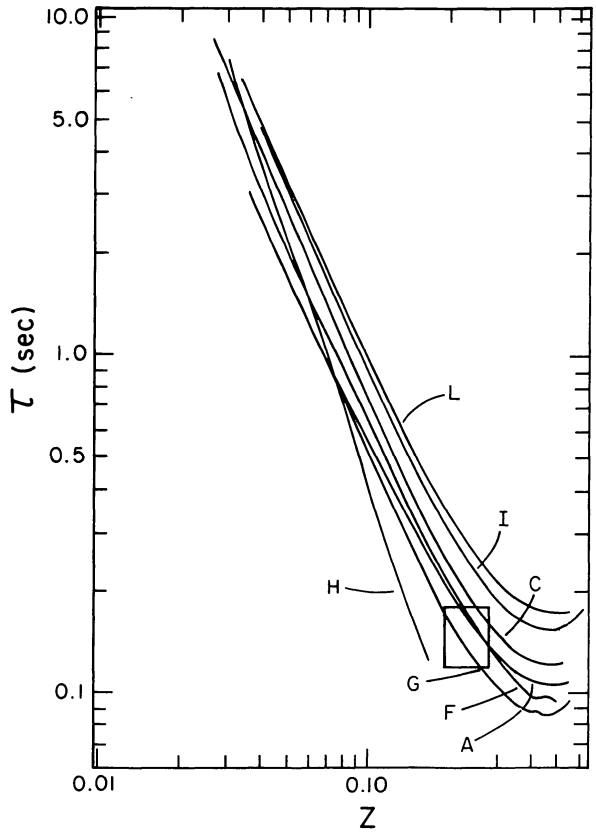

FIG. 7.—The gravitational radiation damping time τ for the quadrupole mode is illustrated as a function of surface redshift z for neutron stars constructed from equations of state A, C, F–L. The box gives the values of the redshift and decay time for the 1979 March 5 γ-ray burst event.

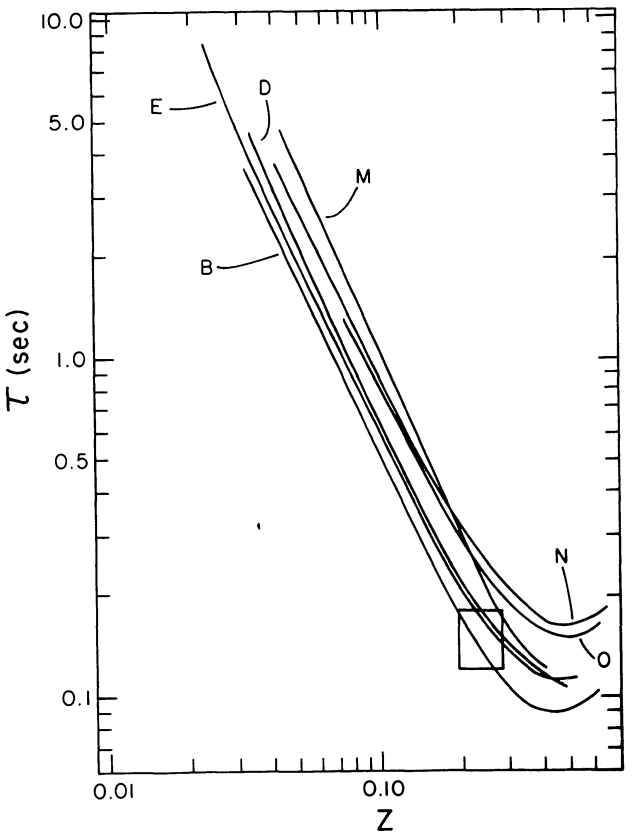

FIG. 8.—The gravitational radiation damping time τ for the quadrupole mode is illustrated as a function of surface redshift z for neutron stars constructed from equations of state B, D, E, M–O. The box gives the values of the redshift and decay time for the 1979 March 5 γ-ray burst event.

equations of state considered here have very uniform ranges in the redshift parameter: $z \approx 0.02$ for the low mass limit and $z \approx 0.5$ for the high mass limit.

The properties of the quadrupole mode having no radial nodes is described here in terms of five parameters: T, τ, E, d_r, and d_θ. The first two parameters T and τ describe the frequency of the mode. These parameters are related to the eigenfrequency ω by the relationship

$$T = 2\pi/\mathrm{Re}\,(\omega), \tag{2}$$

$$\tau = 1/\mathrm{Im}\,(\omega). \tag{3}$$

We tabulate T in units of milliseconds, while τ is given in units of seconds. The two parameters d_r and d_θ are used to describe qualitatively the behavior of the two fluid eigenfunctions $W(r)$ and $V(r)$ (see Appendix A). The parameter d_r gives the average radial motion of the surface of the star, normalized by the radial motion of the fluid at the center of the star. Thus, d_r is related to the radial function $W(r)$ by

$$d_r = (1-2M/R)^{1/2} W(R)/W(0). \tag{4}$$

Similarly, the parameter d_θ describes the average angular displacement of the fluid on the surface of the stellar model, normalized by the value of the angular motion at the center of the star. Thus, d_θ is related to the function $V(r)$ by

$$d_\theta = V(R)/V(0). \tag{5}$$

Finally, the parameter E measures the kinetic energy stored in the pulsation of this mode of the star. The amplitude of the pulsation is normalized by the average radial displacement of the fluid at the surface of the star in this mode. This parameter is tabulated in units of 10^{53} ergs, and corresponds to a mode with average radial motion equal to the radius of the star. For a mode with a smaller amplitude, say the average radial displacement being ε times the radius of the star, the tabulated entry must be multiplied by ε^2 to obtain the appropriate pulsation energy. The pulsation energy E of this mode is related to the other parameters of the star by the expression (see the Appendix for details):

$$E = \pi\tau \left| \frac{\beta(\mathrm{Re}\,\omega)}{8TW(R)} \right|^2 \frac{(l+2)!}{(l-2)!} e^{\lambda(R)}. \tag{6}$$

The function $\beta(\omega)$ in equation (6) is the amplitude of the outgoing gravitational radiation (see eq. [A41]). The parameters d_r, d_θ, and E are discussed more fully by Thorne (1969*a*), where careful derivations of equations (4)–(6) may be found.

Figures 5 and 6 depict the dependence of the oscillation frequency $2\pi/T$ on the surface redshift z of the neutron star models considered here. Similarly, Figures 7 and 8 depict the dependence of the damping time τ on the surface redshift z. It is interesting to note that the ordering of the curves on these graphs essentially mimics the ordering of these equations of state by "average stiffness." The ordering based on stiffness is (roughly) H < G < B < F < D < A < E < C < M < O < I < N < L, where H is the softest and L the stiffest equation of state. We see these same orderings qualitatively followed by the frequency and damping time curves. The softest equations of state have the highest frequencies (for given redshift) and the shortest damping times. The softer equations of state have more centrally condensed stellar models with larger average densities. Consequently, these models have shorter dynamical time scales and thus higher pulsation frequencies. The models having softer equations of state are more relativistic (higher surface redshift) and consequently are more effective emittors of gravitational radiation.

An interesting semiempirical result can be seen in Figures 7 and 8. For small enough values of the surface redshift, $z < 0.2$, the gravitational radiation damping time is related to the surface redshift by the following power law: $\tau \approx z^{-1.7}$. The power is essentially independent of the equation of state. We have not yet been able

TABLE 3

QUADRUPOLE OSCILLATIONS OF NEUTRON STARS (equation of state A)

ρ_c (10^{15} g cm^{-3})	R (km)	$M/M_\odot$	Z	T (10^{-3} s)	τ (s)	E (10^{54} ergs)	d_r	d_θ
5.012	8.065	1.644	0.585	0.3074	0.1126	12.22	2.1	3.6
3.981	8.426	1.653	0.542	0.3234	0.1074	11.58	1.8	3.0
3.388	8.685	1.642	0.505	0.3362	0.1067	10.90	1.7	2.6
3.000	8.887	1.620	0.472	0.3466	0.1059	10.03	1.6	2.4
2.344	9.273	1.535	0.399	0.3703	0.1091	7.89	1.4	2.0
1.995	9.495	1.447	0.349	0.3882	0.1168	6.35	1.4	1.8
1.778	9.640	1.365	0.311	0.4028	0.1268	5.20	1.3	1.7
1.698	9.694	1.328	0.296	0.4086	0.1306	4.79	1.3	1.7
1.585	9.763	1.271	0.275	0.4182	0.1404	4.18	1.3	1.6
1.514	9.800	1.231	0.261	0.4251	0.1492	3.85	1.3	1.6
1.259	9.927	1.050	0.206	0.4544	0.1964	2.45	1.3	1.4
1.000	9.997	0.810	0.147	0.4945	0.3144	1.20	1.3	1.3
0.891	10.010	0.690	0.120	0.5161	0.4230	0.77	1.4	1.3
0.800	10.035	0.581	0.098	0.5366	0.5805	0.46	1.5	1.3
0.708	10.121	0.464	0.075	0.5614	0.8793	0.22	1.7	1.3
0.600	11.244	0.260	0.036	0.6541	3.0132	0.01	4.0	2.0

TABLE 4

QUADRUPOLE OSCILLATIONS OF NEUTRON STARS (equation of state B)

ρ_c (10^{15} g cm^{-3})	R (km)	$M/M_\odot$	Z	T (10^{-3} s)	τ (s)	E (10^{54} ergs)	d_r	d_θ
7.943	6.661	1.397	0.621	0.2510	0.1051	10.17	2.4	4.3
6.200	7.002	1.412	0.573	0.2647	0.0986	9.72	2.1	3.5
5.012	7.313	1.403	0.519	0.2776	0.0926	8.71	1.9	2.9
3.981	7.684	1.360	0.447	0.2946	0.0896	7.25	1.7	2.4
3.388	7.950	1.303	0.392	0.3090	0.0914	5.94	1.6	2.2
3.020	8.131	1.250	0.353	0.3204	0.0955	5.04	1.5	2.0
3.000	8.141	1.247	0.351	0.3207	0.0947	5.05	1.5	2.0
2.630	8.342	1.171	0.307	0.3360	0.1045	3.99	1.5	1.8
1.995	8.760	0.970	0.219	0.3763	0.1468	2.14	1.5	1.6
1.259	9.506	0.638	0.117	0.4756	0.3882	0.61	1.5	1.4
1.000	9.831	0.522	0.089	0.5248	0.6375	0.32	1.6	1.4
0.891	9.971	0.473	0.078	0.5454	0.7997	0.24	1.7	1.4
0.800	10.071	0.436	0.071	0.5597	0.9552	0.18	1.8	1.4
0.708	10.208	0.390	0.062	0.5762	1.2031	0.12	2.0	1.4
0.600	11.512	0.244	0.033	0.6692	3.5401	0.01	4.9	2.3
0.500	15.045	0.167	0.017	0.8859	35.1410	0.00	200.9	52.2

TABLE 5

QUADRUPOLE OSCILLATIONS OF NEUTRON STARS (equation of state C)

ρ_c (10^{15} g cm^{-3})	R (km)	$M/M_\odot$	Z	T (10^{-3} s)	τ (s)	E (10^{54} ergs)	d_r	d_θ
3.548	9.604	1.845	0.520	0.3610	0.1235	10.92	2.2	3.4
3.000	9.955	1.852	0.490	0.3770	0.1214	10.59	2.0	3.0
2.512	10.315	1.840	0.454	0.3947	0.1211	9.87	1.8	2.6
2.239	10.547	1.821	0.428	0.4068	0.1221	9.23	1.7	2.4
1.995	10.777	1.790	0.401	0.4201	0.1245	8.53	1.6	2.2
1.778	11.015	1.746	0.371	0.4346	0.1289	7.52	1.6	2.1
1.585	11.237	1.689	0.341	0.4496	0.1342	6.72	1.5	2.0
1.413	11.446	1.619	0.311	0.4670	0.1456	5.78	1.5	1.9
1.259	11.647	1.533	0.279	0.4859	0.1605	4.89	1.4	1.7
1.122	11.836	1.435	0.248	0.5067	0.1817	3.95	1.4	1.6
1.000	12.020	1.322	0.217	0.5311	0.2138	3.11	1.4	1.6
0.800	12.335	1.094	0.164	0.5849	0.3189	1.81	1.4	1.4
0.600	12.712	0.809	0.110	0.6687	0.6247	0.77	1.5	1.3
0.500	12.988	0.652	0.084	0.7297	1.0257	0.42	1.5	1.3
0.400	13.450	0.489	0.058	0.8130	2.0026	0.17	1.8	1.3
0.320	14.244	0.359	0.039	0.9090	4.1862	0.05	2.4	1.5
0.260	15.557	0.266	0.026	1.0091	8.6376	0.01	4.6	2.2

TABLE 6

QUADRUPOLE OSCILLATIONS OF NEUTRON STARS (equation of state D)

ρ_c (10^{15} g cm^{-3})	R (km)	$M/M_\odot$	Z	T (10^{-3} s)	τ (s)	E (10^{54} ergs)	d_r	d_θ
3.981	9.040	1.645	0.470	0.3407	0.1063	8.71	2.1	3.1
3.548	9.261	1.650	0.453	0.3522	0.1087	8.52	2.0	2.9
3.000	9.598	1.648	0.424	0.3700	0.1109	8.29	1.8	2.5
2.512	9.947	1.631	0.392	0.3900	0.1152	7.33	1.7	2.0
2.239	10.154	1.610	0.371	0.4028	0.1183	7.16	1.5	2.1
1.995	10.336	1.580	0.350	0.4155	0.1233	6.71	1.5	1.9
1.778	10.450	1.547	0.333	0.4245	0.1277	6.25	1.4	1.8
1.548	10.561	1.497	0.312	0.4346	0.1342	5.62	1.4	1.8
1.413	10.678	1.424	0.284	0.4480	0.1470	4.69	1.4	1.7
1.259	10.829	1.312	0.248	0.4672	0.1686	3.67	1.4	1.6
1.122	10.966	1.186	0.212	0.4899	0.2024	2.71	1.4	1.5
1.000	11.088	1.060	0.180	0.5141	0.2511	1.95	1.4	1.5
0.800	11.301	0.820	0.128	0.5679	0.4223	0.96	1.4	1.4
0.600	11.697	0.549	0.077	0.6542	1.0054	0.27	1.7	1.4
0.500	12.189	0.413	0.054	0.7227	1.9273	0.10	2.0	1.4
0.400	13.355	0.290	0.034	0.8267	4.5730	0.02	3.5	1.8
0.320	15.472	0.211	0.021	0.9518	10.9460	0.00	13.5	4.7

TABLE 7

QUADRUPOLE OSCILLATIONS OF NEUTRON STARS (equation of state E)

ρ_c (10^{15} g cm^{-3})	R (km)	$M/M_\odot$	Z	T (10^{-3} s)	τ (s)	E (10^{54} ergs)	d_r	d_θ
3.070	9.018	1.730	0.519	0.3486	0.1128	11.71	1.7	2.7
2.818	9.174	1.711	0.492	0.3560	0.1112	10.90	1.6	2.5
2.512	9.368	1.675	0.456	0.3665	0.1105	9.90	1.5	2.3
1.778	9.917	1.474	0.335	0.4054	0.1233	6.12	1.4	1.8
1.585	10.070	1.376	0.295	0.4214	0.1357	4.85	1.4	1.7
1.413	10.202	1.265	0.256	0.4392	0.1550	3.76	1.3	1.6
1.259	10.316	1.144	0.220	0.4592	0.1844	2.79	1.3	1.5
1.000	10.499	0.891	0.155	0.5058	0.2951	1.38	1.4	1.4
0.794	10.694	0.651	0.104	0.5628	0.5575	0.57	1.5	1.3
0.631	11.074	0.452	0.066	0.6328	1.2200	0.17	1.8	1.4
0.501	11.963	0.305	0.040	0.7210	2.6917	0.03	2.9	1.7
0.398	14.042	0.206	0.022	0.8431	8.3408	0.00	12.2	4.3

to understand why the damping time should scale in this way. For larger values of the redshift parameter, $z > 0.2$, all of the curves in Figures 7 and 8 curve upward. This occurs, we believe, because the emission of gravitational radiation becomes impeded for very compact models due to the backscattering of the waves by the deep gravitational potential well.

IV. DISCUSSION

Our initial interest in these calculations was motivated by the suggestion of Ramaty *et al.* (1980) that many features of the 1979 March 5 γ-ray burst event could be understood by assuming the source was an oscillating neutron star. The source has been identified with the supernova remnant N49 (located in the Large Magellanic Cloud) by its position (see Evans *et al.* 1980). Furthermore, Liang (1981) has shown that the spectrum of this source is consistent with synchrotron radiation in a 1.9×10^{11} gauss magnetic field modified by inverse Compton scattering. Liang calculates the total luminosity of such a source to be $\sim 2.5\times10^{44}$ ergs s^{-1} which is in remarkable agreement with the observed burst luminosity if a Large Magellanic Cloud origin is assumed. In addition to the continuum spectrum considered, there is an emission line whose peak lies at ~ 430 keV. This line has been interpreted as the 511 keV $e^+ - e^-$ annihilation line whose peak has been blueshifted by ~ 20 keV due to finite temperature effects (see Ramaty and Meszaros 1981) and redshifted by the gravitational field of the source. With this interpretation, the resulting gravitational redshift has the value $z = 0.23$ with an uncertainty of ~ 0.05. This redshift is

TABLE 8

QUADRUPOLE OSCILLATIONS OF NEUTRON STARS (equation of state F)

ρ_c (10^{15} g cm^{-3})	R (km)	$M/M_\odot$	Z	T (10^{-3} s)	τ (s)	E (10^{54} ergs)	d_r	d_θ
5.012	7.935	1.462	0.481	0.2927	0.0961	7.52	2.2	3.3
4.850	8.006	1.462	0.473	0.2963	0.0977	7.31	2.2	3.3
4.677	8.088	1.460	0.464	0.2999	0.0974	6.97	2.2	3.2
4.560	8.146	1.459	0.457	0.3023	0.0973	6.79	2.2	3.2
4.467	8.188	1.458	0.452	0.3043	0.0971	7.06	2.1	3.0
4.266	8.294	1.455	0.440	0.3087	0.0958	6.95	2.1	2.9
3.981	8.455	1.448	0.422	0.3162	0.0957	6.76	2.0	2.7
3.548	8.746	1.432	0.391	0.3315	0.0998	6.12	1.9	2.5
3.162	9.042	1.411	0.362	0.3478	0.1040	5.59	1.8	2.3
2.818	9.349	1.385	0.333	0.3666	0.1113	4.06	2.0	2.5
2.512	9.642	1.357	0.308	0.3851	0.1187	4.70	1.6	2.0
2.239	9.864	1.330	0.289	0.4022	0.1294	4.06	1.6	1.9
1.995	10.046	1.300	0.272	0.4163	0.1383	4.23	1.4	1.7
1.778	10.220	1.263	0.255	0.4310	0.1492	3.68	1.4	1.7
1.585	10.364	1.218	0.238	0.4469	0.1655	3.19	1.4	1.6
1.413	10.505	1.165	0.220	0.4619	0.1824	2.96	1.3	1.5
1.259	10.636	1.099	0.200	0.4798	0.2090	2.62	1.3	1.4
1.122	10.762	1.021	0.179	0.5002	0.2457	2.00	1.3	1.4
1.000	10.868	0.938	0.159	0.5214	0.2956	1.54	1.3	1.4
0.794	11.046	0.752	0.119	0.5687	0.4709	0.87	1.3	1.2
0.631	11.249	0.560	0.083	0.6247	0.8737	0.36	1.4	1.1
0.501	12.546	0.306	0.038	0.7794	3.2171	0.03	2.0	1.1
0.398	13.647	0.242	0.027	0.8621	6.7137	0.01	3.3	1.5
0.316	14.899	0.200	0.020	0.9259	10.9830	0.00	13.0	4.5

TABLE 9

QUADRUPOLE OSCILLATIONS OF NEUTRON STARS (equation of state G)

ρ_c (10^{15} g cm^{-3})	R (km)	$M/M_\odot$	Z	T (10^{-3} s)	τ (s)	E (10^{54} ergs)	d_r	d_θ
6.310	6.944	1.357	0.538	0.2606	0.0920	8.34	2.1	3.4
6.042	7.013	1.356	0.527	0.2634	0.0910	8.17	2.0	3.2
5.232	7.236	1.348	0.491	0.2726	0.0870	7.66	1.9	2.9
4.503	7.471	1.327	0.450	0.2834	0.0858	6.80	1.8	2.6
4.161	7.600	1.310	0.427	0.2902	0.0875	6.41	1.7	2.4
3.829	7.742	1.286	0.401	0.2973	0.0875	5.88	1.7	2.3
3.498	7.899	1.253	0.372	0.3067	0.0909	5.26	1.6	2.2
3.198	8.061	1.214	0.342	0.3169	0.0950	4.55	1.6	2.1
2.912	8.228	1.168	0.312	0.3282	0.1001	4.01	1.5	1.9
2.631	8.398	1.114	0.282	0.3419	0.1107	3.39	1.5	1.8
2.376	8.558	1.057	0.255	0.3559	0.1230	2.83	1.5	1.7
2.239	8.638	1.025	0.241	0.3634	0.1310	2.55	1.5	1.7
1.995	8.781	0.958	0.215	0.3789	0.1505	2.03	1.5	1.6
1.778	8.943	0.877	0.186	0.3979	0.1805	1.56	1.5	1.6
1.585	9.136	0.786	0.158	0.4236	0.2334	1.11	1.5	1.5
1.413	9.333	0.705	0.134	0.4503	0.3027	0.81	1.5	1.4
1.259	9.506	0.638	0.117	0.4757	0.3892	0.61	1.5	1.4
1.122	9.679	0.575	0.101	0.5017	0.5033	0.44	1.6	1.4
1.000	9.833	0.522	0.089	0.5248	0.6375	0.32	1.6	1.4
0.794	10.081	0.433	0.070	0.5606	0.9654	0.17	1.8	1.4
0.631	10.922	0.282	0.040	0.6324	2.4649	0.02	3.3	1.8

TABLE 10

QUADRUPOLE OSCILLATIONS OF NEUTRON STARS (equation of state H)

ρ_c (10^{15} g cm^{-3})	R (km)	$M/M_\odot$	Z	T (10^{-3} s)	τ (s)	E (10^{54} ergs)	d_r	d_θ
10.000	7.474	0.666	0.165	0.2641	0.1291	0.24	6.2	4.5
6.000	8.396	0.682	0.147	0.3101	0.1652	0.25	5.1	3.6
3.000	10.178	0.660	0.112	0.4109	0.3004	0.20	4.2	2.8
1.000	14.146	0.553	0.063	0.6814	1.2828	0.08	4.2	2.4
0.300	20.811	0.404	0.030	1.1967	7.4287	0.01	7.5	3.1

TABLE 11

QUADRUPOLE OSCILLATIONS OF NEUTRON STARS (equation of state I)

ρ_c (10^{15} g cm^{-3})	R (km)	$M/M_\odot$	Z	T (10^{-3} s)	τ (s)	E (10^{54} ergs)	d_r	d_θ
2.239	11.660	2.443	0.619	0.4496	0.1760	20.24	2.0	3.6
1.995	11.906	2.446	0.595	0.4599	0.1693	19.60	1.9	3.3
1.778	12.194	2.439	0.563	0.4723	0.1628	18.73	1.7	2.9
1.585	12.472	2.418	0.530	0.4852	0.1579	17.36	1.6	2.7
1.413	12.750	2.380	0.493	0.4986	0.1522	16.03	1.6	2.4
1.259	13.027	2.324	0.454	0.5151	0.1543	14.22	1.5	2.2
1.122	13.282	2.249	0.414	0.5317	0.1568	12.41	1.4	2.1
1.000	13.502	2.154	0.375	0.5488	0.1614	10.56	1.4	1.9
0.794	13.887	1.892	0.294	0.5924	0.1935	6.94	1.3	1.7
0.631	14.130	1.561	0.218	0.6459	0.2670	3.99	1.3	1.5
0.501	14.228	1.207	0.155	0.7100	0.4319	2.01	1.3	1.3
0.398	14.273	0.870	0.104	0.7870	0.8264	0.85	1.4	1.3
0.316	14.443	0.590	0.066	0.8779	1.8385	0.28	1.5	1.3
0.251	15.115	0.380	0.039	0.9861	4.6943	0.06	2.2	1.4
0.199	17.359	0.235	0.021	1.1290	14.0900	0.00	8.9	3.4

TABLE 12

QUADRUPOLE OSCILLATIONS OF NEUTRON STARS (equation of state L)

ρ_c (10^{15} g cm^{-3})	R (km)	$M/M_\odot$	Z	T (10^{-3} s)	τ (s)	E (10^{54} ergs)	d_r	d_θ
1.585	13.514	2.659	0.545	0.5288	0.1738	20.40	1.7	2.8
1.500	13.616	2.661	0.538	0.5335	0.1708	20.33	1.6	2.7
1.413	13.734	2.660	0.529	0.5402	0.1727	19.98	1.6	2.6
1.259	13.938	2.648	0.510	0.5514	0.1718	19.33	1.5	2.4
1.122	14.129	2.622	0.488	0.5624	0.1712	18.28	1.4	2.3
1.000	14.304	2.579	0.462	0.5735	0.1713	16.93	1.4	2.1
0.891	14.496	2.498	0.427	0.5886	0.1735	15.09	1.3	2.0
0.794	14.685	2.391	0.388	0.6042	0.1774	10.47	1.4	2.1
0.631	14.992	2.044	0.294	0.6525	0.2158	7.81	1.2	1.6
0.600	15.025	1.959	0.275	0.6640	0.2296	6.93	1.2	1.5
0.501	15.058	1.640	0.214	0.7071	0.3045	4.27	1.2	1.4
0.500	15.057	1.635	0.213	0.7077	0.3058	4.24	1.2	1.4
0.400	14.895	1.226	0.149	0.7655	0.5003	2.02	1.2	1.3
0.398	14.889	1.214	0.148	0.7672	0.5084	1.97	1.2	1.3
0.318	14.656	0.762	0.087	0.8546	1.2029	0.59	1.4	1.2
0.300	14.647	0.668	0.075	0.8803	1.5543	0.41	1.4	1.2
0.251	14.960	0.439	0.046	0.9668	3.6044	0.10	1.9	1.3
0.224	15.614	0.331	0.033	1.0322	6.5092	0.03	2.8	1.6
0.200	16.920	0.251	0.023	1.1081	12.0160	0.00	6.3	2.6
0.199	16.958	0.250	0.022	1.1099	12.1910	0.00	6.5	2.7

TABLE 13

QUADRUPOLE OSCILLATIONS OF NEUTRON STARS (equation of state M)

ρ_c (10^{15} g cm^{-3})	R (km)	$M/M_\odot$	Z	T (10^{-3} s)	τ (s)	E (10^{54} ergs)	d_r	d_θ
3.162	10.913	1.753	0.379	0.3959	0.1251	5.20	2.8	3.5
2.239	11.908	1.759	0.332	0.4452	0.1372	4.97	2.3	2.8
1.778	12.648	1.736	0.297	0.4877	0.1556	4.58	2.1	2.5
1.585	13.044	1.718	0.279	0.5121	0.1676	4.33	2.0	2.3
1.259	13.830	1.670	0.247	0.5661	0.2003	3.91	1.8	2.0
1.000	14.589	1.612	0.218	0.6261	0.2467	3.46	1.6	1.8
0.794	15.281	1.547	0.194	0.6896	0.3091	3.07	1.5	1.6
0.708	15.475	1.519	0.187	0.7102	0.3342	2.92	1.4	1.5
0.631	15.648	1.483	0.178	0.7308	0.3639	2.73	1.4	1.5
0.562	15.796	1.437	0.169	0.7513	0.3993	2.52	1.4	1.5
0.501	15.922	1.382	0.160	0.7716	0.4413	2.26	1.4	1.4
0.398	16.095	1.231	0.137	0.8155	0.5740	1.67	1.4	1.4
0.316	16.368	0.931	0.096	0.9092	1.0608	0.78	1.4	1.3
0.251	16.754	0.681	0.066	1.0162	2.1414	0.32	1.6	1.3
0.199	17.464	0.485	0.044	1.1385	4.6651	0.10	2.0	1.4
0.158	18.979	0.337	0.027	1.2840	10.9580	0.02	3.6	1.8

TABLE 14

QUADRUPOLE OSCILLATIONS OF NEUTRAON STARS (equation of state N)

ρ_c (10^{15} g cm^{-3})	R (km)	$M/M_\odot$	Z	T (10^{-3} s)	τ (s)	E (10^{54} ergs)	d_r	d_θ
3.000	11.544	2.485	0.657	0.4462	0.1832	22.53	2.3	4.3
2.000	12.270	2.563	0.616	0.4807	0.1772	23.07	1.8	3.2
1.500	12.825	2.561	0.561	0.5076	0.1676	21.46	1.5	2.6
1.000	13.472	2.370	0.443	0.5478	0.1618	15.07	1.3	2.0
0.900	13.653	2.243	0.394	0.5645	0.1655	12.39	1.3	1.8
0.800	13.800	2.080	0.342	0.5855	0.1781	9.81	1.2	1.7
0.700	13.883	1.871	0.289	0.6119	0.2058	7.14	1.2	1.6
0.600	13.879	1.608	0.233	0.6434	0.2573	4.70	1.2	1.4
0.550	13.823	1.452	0.204	0.6618	0.3017	3.61	1.2	1.4
0.500	13.719	1.278	0.175	0.6822	0.3701	2.61	1.2	1.3
0.450	13.544	1.057	0.140	0.7098	0.5074	1.61	1.2	1.3
0.400	13.338	0.801	0.102	0.7496	0.8233	0.79	1.3	1.2
0.350	13.242	0.567	0.070	0.8000	1.5548	0.30	1.5	1.2
0.300	13.634	0.362	0.042	0.8721	3.7229	0.06	2.2	1.4

TABLE 15

QUADRUPOLE OSCILLATIONS OF NEUTRON STARS (equation of state O)

ρ_c (10^{15} g cm^{-3})	R (km)	$M/M_\odot$	Z	T (10^{-3} s)	τ (s)	E (10^{54} ergs)	d_r	d_θ
2.365	11.292	2.374	0.624	0.4407	0.1618	21.76	1.8	3.2
2.000	11.583	2.380	0.595	0.4539	0.1555	21.05	1.7	2.9
1.780	11.785	2.370	0.569	0.4652	0.1560	20.10	1.6	2.6
1.500	12.080	2.327	0.523	0.4800	0.1487	18.07	1.4	2.3
1.259	12.364	2.235	0.465	0.4987	0.1488	15.14	1.3	2.1
1.000	12.671	2.013	0.372	0.5284	0.1577	10.41	1.3	1.8
0.800	12.834	1.682	0.277	0.5672	0.1944	6.08	1.2	1.5
0.750	12.840	1.567	0.250	0.5815	0.2169	5.01	1.2	1.5
0.668	12.822	1.361	0.207	0.6080	0.2706	3.41	1.2	1.4
0.639	12.799	1.282	0.192	0.6191	0.3003	2.93	1.2	1.4
0.631	12.791	1.260	0.188	0.6221	0.3092	2.79	1.2	1.4
0.562	12.703	1.065	0.153	0.6508	0.4140	1.82	1.2	1.3
0.500	12.584	0.886	0.124	0.6788	0.5727	1.15	1.2	1.3
0.450	12.461	0.742	0.101	0.7017	0.7826	0.72	1.3	1.2
0.400	12.335	0.555	0.074	0.7340	1.3026	0.32	1.5	1.3
0.350	12.637	0.345	0.043	0.7918	3.1435	0.06	2.2	1.4
0.300	15.438	0.187	0.018	0.9275	13.5140	0.00	36.0	10.6

completely consistent with the surface redshift from a 1.2 to 1.4 $M_\odot$ neutron star remnant of a supernova (see Figs. 3 and 4). All of these considerations taken together make it appear quite likely that the source of the 1979 March 5 γ-ray burst event is on or near a neutron star.

The initial burst of the 1979 March 5 event had a characteristic rise time shorter than 0.2 ms; the burst then decayed exponentially with a time constant of 150 ± 30 ms for an initial period of ~ 100 ms; this initial period was followed by a steeper exponential decay having time constant of ~ 35 ms. The decay times for this pulse are far too long to be accounted for in terms of the cooling of the $e^+ - e^-$ pairs by synchrotron emission (10^{-15} s; Liang 1981) or the pair annihilation time (10^{-12} s; Ramaty *et al.* 1980) for the type of atmosphere which successfully models the spectrum of the burst. These considerations lead Ramaty *et al.* (1980) to suggest that the energy source for the burst might be the oscillations of the associated neutron star. They suggest that the star could be set into oscillation by some internal event: a phase transition in the core, for example. The resulting oscillations might heat the atmosphere to temperatures hot enough to create the $e^+ - e^-$ pairs through the strong magnetic fields which are tied to the star. The dominant energy loss mechanism for such an event might be the emission of gravitational radiation by the quadrupole mode, they suggest. Thus, the 150 ms exponential decay phase, during which most of the observed energy was released, might be a measure of the gravitational wave damping time for this object. This model can now be checked for consistency using the results of our present computations of the quadrupole modes of realistic neutron stars. The observed redshift and the 150 ms decay time of the 1979 March 5 γ-ray event is shown in Figures 7 and 8. We see that these numbers are consistent with the quadrupole damping times of several of the softer equations of state: A, B, D, E, F, G. From Figures 3 and 4 we see that the observed surface redshift is consistent for models A, D, E, F with masses that could have resulted from the collapse of a 1.4 $M_\odot$ core. The masses of stars from models B and G appear to be too small to be consistent with the observed redshift and the standard picture of neutron star formation. The oscillation period of the quadrupole mode for these models can be inferred from Figures 5 and 6 to be in the range 0.44–0.53 ms. Weisekopf *et al.* (1981) have analyzed the meager data which had sufficient time resolution to detect such oscillations (255 events during the first 56 ms of the burst) without finding any evidence for such oscillations.

While the oscillating neutron star model of the 1979 March 5 γ-ray burst event does not yet explain all of the observed features (e.g., the 35 ms decay time, the 8 s periodicity, or the 50 s long decay rate), it does appear to be consistent with the extensive analysis of the quadrupole oscillations of neutron stars which we have prepared here.

The other class of observations which may be related to oscillating neutron stars is the micropulse structure of pulsars. A 0.9 ms periodicity in the pulsations of PSR 2016+28 was first noted by Boriakoff (1976). Since then periodicities in the 1 ms range have been observed in other objects by a number of authors: Cordes (1976), Cordes and Hankins (1977), Hankins and Boriakoff (1978), and Soglasnov *et al.* (1981). Boriakoff (1976) suggested that the 0.9 ms periodicity which he observed might be caused by a nonradial oscillation of the neutron star. Cordes (1976) notes that the micropulse structure in these objects becomes uncorrelated between subpulses whose separation is larger than ~ 10 ms. Since the damping time of the nonradial modes by gravitational radiation emission is much longer than 10 ms, Cordes concluded that it was not reasonable to associate the micropulses with neutron star oscillations.

Our computations of neutron star damping times by gravitational radiation emission give times in the range 100–300 ms for neutron stars in the expected mass range. Higher order modes are expected to have even longer damping times. We agree with Cordes (1976), therefore, that nonradial oscillations of neutron stars whose primary damping mechanism is gravitational radiation do not provide a consistent model for the micropulses. Even if other damping mechanisms were present which were more efficient than gravitational radiation in damping the neutron star oscillations, it does not appear to us that such a model could be consistent with these observations. The 0.9 ms period observed in the micropulsations is longer than the 0.8–0.3 ms range of periodicities for the equations of state studied here. To find a quadrupole oscillation period as long as 0.9 ms, the neutron star would have to have a significantly smaller mass than that expected for a collapsed white dwarf core. The most massive star with a period this long has $M/M_\odot = 0.9$, from equation of state M. The expected core mass for this equation of state is 1.35 $M_\odot$ (see Arnett and Bowers 1977). Since the higher order nonradial p modes are expected to have even shorter oscillation periods than those computed here, it seems unlikely to us that these pulsar micropulsations can be modeled as nonradial p mode oscillations of the neutron star. We will argue in the accompanying paper (Glass and Lindblom 1983) that the radial oscillations for these stars also have periods which are too short to account for the micropulsations. Our analysis does not rule out the possibility that a dipole mode could have an appropriate frequency, or that a mode associated with the nonperfect fluid properties of neutron star matter (the nonadiabatic g modes or the tortional modes of the solid crust) could have appropriate frequencies to describe the micropulsations.

APPENDIX A

HOW TO COMPUTE THE QUASI-NORMAL MODES

In this appendix we describe the technical details involved in the calculation of the quasi-normal modes of general relativistic neutron star models. The techniques described here for determining the perturbation functions within the star are closely related to those described by Thorne (1969*a*, *b*). The method described here for determining the eigenfrequency of a particular mode is closely related to the techniques developed by Detweiler (1980) in his analysis of the modes of the Kerr black hole.

I. THE EQUILIBRIUM STELLAR MODEL

The calculation of the pulsation of a stellar model must begin with the numerical determination of the equilibrium stellar model itself. The general static spherical metric which describes the geometry of an equilibrium stellar model can be written as

$$ds^2 = -e^{\nu}\,dt^2 + e^{\lambda}\,dr^2 + r^2\left(d\theta^2 + \sin^2\theta\,d\phi^2\right), \tag{A1}$$

where ν and λ are functions of r. It is convenient to define the function $M(r)$ as follows:

$$M(r) = \tfrac{1}{2}r(1 - e^{-\lambda}). \tag{A2}$$

Einstein's equations for this system are equivalent to the Tolman-Oppenheimer-Volkoff equations, given by

$$\frac{dM}{dr} = 4\pi r^2 \rho, \tag{A3}$$

$$\frac{d\nu}{dr} = 2\frac{M + 4\pi r^3 p}{r(r - 2M)}, \tag{A4}$$

$$\frac{dp}{dr} = -\frac{1}{2}(\rho + p)\frac{d\nu}{dr}. \tag{A5}$$

The functions ρ and p in these equations are the energy density and the pressure of the fluid in the star. The pressure and density are related by an equation of state $\rho = \rho(p)$. These equations are integrated numerically as an initial value problem from the center of the star $r = 0$. The mass function must vanish at the center of the star, $M(0) = 0$, while the values of p and ν may be freely specified here. The equations are then integrated to the value of r where the pressure vanishes $p(R) = 0$. This surface $r = R$ is the surface of the star. The total mass of the star is given by $M(R)$, and the arbitrary constant in the function ν is fixed by normalizing the time coordinate at spatial infinity:

$$e^{\nu(R)} = 1 - 2M(R)/R. \tag{A6}$$

In our numerical calculations, equations (A3)–(A5) were integrated by the Hamming's predictor-corrector-modifier algorithm (see Lambert 1973). The predictor-corrector-modifier algorithm was started using Ralston's (1962) minimal error Runge-Kutta algorithm. The equations were integrated on a uniform radial grid with approximately 350–400 grid points in the internal $(0, R)$. The numerical integration was terminated at the last grid point having a positive pressure. The actual surface of the star was located by matching an analytic polytropic "atmosphere" onto this last numerical gridpoint. The density and pressure near the surface of a polytropic star vary as

$$p = a(R - r)^{N+1}, \tag{A7}$$

$$\rho = b(R - r)^{N}, \tag{A8}$$

where N is the polytropic index. The constants a, b, R, and N are determined by requiring that p, ρ, dp/dr, and the adiabatic index $\gamma = 1 + 1/N$ be continuous functions at the final gridpoint. For the computations which we have performed, the surface value of γ is typically in the range 1.3 to 1.4. The accuracy of our computations appear to be at

the level of a few parts in 10^4. Our models are unchanged to this level of accuracy when the number of grid points is doubled in our integrations. Furthermore, our models agree with those computed by Arnett and Bowers (1977) to this level of accuracy.

II. THE PERTURBATIONS INSIDE THE STELLAR MODEL

The perturbations of these static spherical stars are decomposed into appropriate spherical harmonics Y_m^l and sinusoidal time dependence $e^{i\omega t}$. By making an appropriate choice of gauge, the perturbed metric for a given spherical harmonic may be put in the form (see Thorne and Campolattaro 1967):

$$ds^2 = -e^{\nu}\left(1+\mu^l H_0 Y_m^l e^{i\omega t}\right)dt^2 - 2i\omega\mu^l H_1 Y_m^l e^{i\omega t}\,dt\,dr + e^{\lambda}\left(1-\mu^l H_0 Y_m^l e^{i\omega t}\right)dr^2$$
$$+ r^2\left(1-\mu^l K Y_m^l e^{i\omega t}\right)\left(d\theta^2+\sin^2\theta\,d\phi^2\right). \tag{A9}$$

The parameter μ is defined by

$$\mu = \begin{cases} r/R & 0 \le r < R \\ 1 & r \ge R \end{cases}. \tag{A10}$$

The functions H_0, H_1, and K depend only on r. These functions differ from the analogous functions used by Thorne and Campolattaro (1967) by the factors μ^l; by factoring out this r^l dependence, we improve the numerical behavior of our functions near $r=0$.

The perturbations of the fluid variables in the stellar model are determined from the fluid dislocation vector field ξ^α. In an appropriate gauge $\xi^t = 0$, and the other components are given by

$$\xi^r = \mu^l r^{-1} e^{-\lambda/2} W Y_m^l e^{i\omega t}, \tag{A11}$$

$$\xi^\theta = -\mu^l r^{-2} V \partial_\theta Y_m^l e^{i\omega t}, \tag{A12}$$

$$\xi^\phi = -\mu^l (r\sin\theta)^{-2} V \partial_\phi Y_m^l e^{i\omega t}. \tag{A13}$$

The radial functions V and W differ from the analogous functions of Thorne and Campolattaro (1967) by the factor μ^l. We will find it convenient to use a function $X(r)$ rather than $V(r)$ in the perturbation equations; these functions are related by

$$V = \omega^{-2}(\rho+p)^{-1} e^{\nu}\left[e^{-\nu/2}X + r^{-1}p' e^{-\lambda/2}W - \tfrac{1}{2}(\rho+p)H_0\right]. \tag{A14}$$

In these equations the functions $\rho, p, p' = dp/dr$, ν, and λ represent the functions of r from the equilibrium stellar model. Wherever V appears in the following equations, it is to be thought of as this functional of H_0, W, and X.

Einstein's equations for this physical situation have been written out by Thorne and Campolattaro (1967). These equations are given by

$$H_1 = \frac{2}{l(l+1)}\left[r^2K' + r(l+e^{\lambda})K - e^{\lambda}(3M+4\pi r^3 p)K - rH_0 + 8\pi r(\rho+p)e^{\lambda/2}W\right], \tag{A15}$$

$$W' = -(l+1)r^{-1}W + re^{\lambda/2}\left[\gamma^{-1}p^{-1}e^{-\nu/2}X - l(l+1)r^{-2}V + \tfrac{1}{2}H_0 + K\right], \tag{A16}$$

$$X' + \tfrac{1}{2}(\rho+p)e^{\nu/2}(H'-2K') = (\rho+p)\left[-\omega^2 r^{-1}e^{(\lambda-\nu)/2}W + \tfrac{1}{2}e^{\nu/2}r(r^{-2}e^{-\lambda/2}\nu')'W - \tfrac{1}{2}l(l+1)r^{-2}\nu' e^{\nu/2}V\right.$$
$$\left. - \tfrac{1}{2}e^{\nu/2}(lr^{-1}+\tfrac{3}{2}\nu')H_0 + e^{\nu/2}(lr^{-1}+\tfrac{1}{2}\nu')K\right], \tag{A17}$$

$$H_0' + \left[\frac{2\omega^2 r^2}{l(l+1)}e^{-\nu} - 1\right]K' = -lr^{-1}(H_0-K) - e^{\lambda}(2M/r^2 + 8\pi r p)H_0$$
$$- \frac{2\omega^2}{l(l+1)}e^{-\nu}\left[r(l+e^{\lambda})K - e^{\lambda}(3M+4\pi r^3 p)K - rH_0 + 8\pi r(\rho+p)e^{\lambda/2}W\right], \tag{A18}$$

$$H_0' - e^{\lambda}(1-3M/r-4\pi r^2 p)K' - 8\pi\gamma p e^{\lambda/2}W' = (2-l)r^{-1}H_0 - r^{-1}e^{\lambda}\left[1+\tfrac{1}{2}l(l+1)+4\pi r^2(2+\gamma)p\right]H_0 - \omega^2 r e^{\lambda-\nu}K$$
$$+ r^{-1}e^{\lambda}\left[-1+l+\tfrac{1}{2}l(l+1)-3lM/r-4\pi r^2 p(l+2\gamma)\right]K$$
$$+ 8\pi r^{-1}e^{\lambda/2}\left[rp'+(l+1)\gamma p\right]W + 8\pi l(l+1)r^{-1}e^{\lambda}\gamma p V. \quad \text{(A19)}$$

The first of these equations (A15) serves to eliminate H_1 from the system of equations. The four remaining radial perturbation functions H_0, K, W, and X can be thought of as an abstract vector field,

$$\boldsymbol{Y}(r) = \{H_0, K, W, X\}. \quad \text{(A20)}$$

The remaining Einstein's equations for these functions form a first-order linear system of the form

$$\frac{d\boldsymbol{Y}}{dr} = \mathbf{Q}(r, l, \omega)\cdot\boldsymbol{Y}(r). \quad \text{(A21)}$$

The matrix $\mathbf{Q}$ depends on r, l, and the frequency ω, as can be inferred from equations (A16)–(A19).

The radial perturbation equations (A21) form a fourth-order system of linear equations (see Ipser and Thorne 1973). For given values of l and ω it follows that there will exist four linearly independent solutions to these equations inside the stellar model. The physically relevant solutions to these equations must satisfy appropriate boundary conditions. The perturbation functions must be finite everywhere; in particular, the functions must be finite at the boundary $r = 0$. Furthermore, the function X must vanish at the surface of the star $r = R$. This condition, $X(R) = 0$, is equivalent to the physical requirement that the perturbed pressure must vanish on the perturbed surface of the star (see Thorne 1969*a*, *b*). For given values of l and ω there is only one solution which satisfies all of these boundary conditions inside the star.

To determine numerically the unique solution to equation (A21) which satisfies all of the physical boundary conditions, we proceed as follows. At the surface of the star there are three linearly independent vectors $\boldsymbol{Y}(R)$ which satisfy the boundary conditions $X(R) = 0$. We select three such vectors and use them as initial values for the differential equation (A21). We integrate these numerically from $r = R$ back to the "middle" of the star at $r = R/2$. These integrations yield three solutions, $\boldsymbol{Y}_1$, $\boldsymbol{Y}_2$, and $\boldsymbol{Y}_3$, defined on the domain $R \geq r \geq R/2$, each of which satisfy the boundary condition $X(R) = 0$. The unique solution which satisfies all of the boundary conditions must be some constant linear combination of these three solutions in the domain $R \geq r \geq R/2$.

Let us be a bit more explicit about the numerical process of finding the three functions $\boldsymbol{Y}_1$, $\boldsymbol{Y}_2$, and $\boldsymbol{Y}_3$. Recall that the equilibrium stellar model has been determined only on a fixed grid of points. The outermost grid point, having the value $r = R_G$, will never lie precisely on the real surface of the real star at $r = R$. We found in practice that imposing the boundary condition $X(R_G) = 0$ rather than $X(R) = 0$ gave unreliable results (as the grid size was changed, for example). We found it necessary therefore to impose $X(R) = 0$ at the real surface of the star and to calculate what its value at $r = R_G$ must be. Since the outer "atmosphere" of our model was taken to be polytropic (see eqs. [A7]–[A8]), the behavior of the function $X(r)$ in this polytropic region can be evaluated analytically. It follows that

$$X(r) = c(r-R)^{N+1}. \quad \text{(A22)}$$

We choose the boundary conditions for the functions W, H_0, and K at the last grid point $r = R_G$. Using these values, it is straightforward to evaluate $X'(R_G)$ from equation (A21). Using equation (A22), it follows that the value $X(R_G)$ is given by

$$X(R_G) = (N+1)^{-1}(R_G - R)X'(R_G). \quad \text{(A23)}$$

Once this consistent set of boundary values is specified at the last grid point, we integrate numerically using the same algorithms as were described in connection with the equilibrium models.

To complete the solution of the perturbation equations inside the stellar model, we must find the solutions in the domain $0 \leq r \leq R/2$ which are bounded (especially at $r = 0$). The matrix $\boldsymbol{Q}$ in equation (A21) has rather singular behavior at $r = 0$, so it is difficult to determine the solutions to these equations numerically near $r = 0$ in their present form. Rather than transform these equations, we choose to approximate the solutions analytically via a power series expansion about $r = 0$. In Appendix B we describe the results of performing such a power series expansion. We find

that the solution has the form

$$\boldsymbol{Y}(r) = \boldsymbol{Y}(0) + \tfrac{1}{2}\boldsymbol{Y}''(0)\, r^2, \tag{A24}$$

where $\boldsymbol{Y}(0)$ and $\boldsymbol{Y}''(0)$ are constants. By examining the constraints which Einstein's equation places on these constants (see Appendix B) we find that there are two linearly independent solutions which have the form in equation (A24). We can now use this expansion to evaluate the two linearly independent solutions, $\boldsymbol{Y}_4(r)$ and $\boldsymbol{Y}_5(r)$, in some small region near $r = 0$. The error involved in neglecting the higher order terms in the power series expansion is expected to be comparable to $\rho_0^2 r^4$. For the neutron star models which we have computed, the parameters generally satisfy $\rho_0 R^2 \lesssim 0.1$. Consequently, the error in our approximation is expected to be $0.01\ (r/R)^4$. In practice we use the power series expansion only in the domain $0 \le r/R \lesssim 1/25$; consequently, we expect our errors to be only $\sim 10^{-7}$.

To complete the evaluation of the solutions $\boldsymbol{Y}_4$ and $\boldsymbol{Y}_5$, we use the values $\boldsymbol{Y}_4(R/25)$ and $\boldsymbol{Y}_5(R/25)$ from the power series expansion to provide starting values for a normal numerical integration of equation (A21). The numerical integration is continued until $\boldsymbol{Y}_4$ and $\boldsymbol{Y}_5$ are determined everywhere on the domain $0 \le r \le R/2$.

The unique solution to equation (A21) which satisfies all of the boundary conditions must be some constant linear combination of $\boldsymbol{Y}_1$, $\boldsymbol{Y}_2$, and $\boldsymbol{Y}_3$ in the domain $R/2 \le r \le R$. Similarly, this unique solution must be some linear combination of $\boldsymbol{Y}_4$ and $\boldsymbol{Y}_5$ in the region $0 \le r \le R/2$. Thus, the physical solution $\boldsymbol{Y}_p(r)$ must be given by

$$\boldsymbol{Y}_p(r) = \begin{cases} \alpha_1 \boldsymbol{Y}_1(r) + \alpha_2 \boldsymbol{Y}_2(r) + \alpha_3 \boldsymbol{Y}_3(r) & R \ge r \ge R/2 \\ \alpha_4 \boldsymbol{Y}_4(r) + \alpha_5 \boldsymbol{Y}_5(r) & R/2 \ge r \ge 0 \end{cases} \tag{A25}$$

for some constants α_i. To insure the continuity of the physical solution at $r = R/2$, we must impose the condition:

$$\alpha_1 \boldsymbol{Y}_1(R/2) + \alpha_2 \boldsymbol{Y}_2(R/2) + \alpha_3 \boldsymbol{Y}_3(R/2) = \alpha_4 \boldsymbol{Y}_4(R/2) + \alpha_5 \boldsymbol{Y}_5(R/2). \tag{A26}$$

These four equations may be solved for the four independent constants α_i. (The fifth constant represents the freedom to scale the solutions and is arbitrary.)

The procedure outlined above allows us to compute the unique physical solution to equation (A21) for any given values of l and ω.

III. THE PERTURBATIONS OUTSIDE THE STELLAR MODEL

Outside of the stellar model, the perturbation functions which describe the motion of the fluid are no longer defined. The system of perturbation equations reduces therefore to a second-order system of equations for the two metric perturbation quantities H_0 and K. Given a solution to the perturbation equations in the inside of the stellar model, the boundary values $H_0(R)$ and $K(R)$ can be used as initial data to start an integration of the remaining perturbation equations. In this way the functions $H_0(r)$ and $K(r)$ can be determined throughout the region $r \ge R$. An examination of this solution in the region far away from the stellar model will reveal, in general, some mixture of incoming and outgoing gravitational radiation. Thus, a typical value of the frequency ω will not correspond to a resonance of the stellar model; the star must be driven by incoming gravitational radiation to force it to oscillate at this frequency. The frequencies at which the star oscillates freely without incoming gravitational radiation are called the frequencies of the quasi-normal modes of the star. The purpose of this paper is to compute the frequencies of the $l = 2$ quasi-normal modes. It will be necessary therefore to be able to decompose a solution for the perturbed metric into incoming and outgoing gravitational radiation. This decomposition can be accomplished most conveniently in terms of the Zerilli equation (see Zerilli 1970; Fackerell 1971; Chandrasekhar and Detweiler 1975).

The Zerilli function $Z(r^*)$ is defined in terms of the metric perturbations $H_0(r)$ and $K(r)$ by the following transformation:

$$\begin{pmatrix} 0 & 1 \\ a(r) & b(r) \end{pmatrix} \begin{pmatrix} H_0(r) \\ K(r) \end{pmatrix} = \begin{pmatrix} g(r) & 1 \\ h(r) & k(r) \end{pmatrix} \begin{pmatrix} Z(r^*) \\ dZ(r^*)/dr^* \end{pmatrix}, \tag{A27}$$

where $a(r)$, $b(r)$, $g(r)$, $h(r)$, $k(r)$, n, and r^* are defined by

$$a(r) = -(nr + 3M)/\left[\omega^2 r^2 - (n+1)M/r\right], \tag{A28}$$

$$b(r)=\frac{[nr-\omega^2r^4+M(r-3M)]}{(r-2M)[\omega^2r^2-(n+1)M/r]}, \tag{A29}$$

$$g(r)=\frac{[n(n+1)r^2+3nMr+6M^2]}{r^2(nr+3M)}, \tag{A30}$$

$$h(r)=\frac{[-nr^2+3nMr+3M^2]}{(r-2M)(nr+3M)}, \tag{A31}$$

$$k(r)=-r^2/(r-2M), \tag{A32}$$

$$n=\tfrac{1}{2}(l-1)(l+2), \tag{A33}$$

$$r^*=r+2M\log(r/2M-1). \tag{A34}$$

Given the function $Z(r^*)$ which is related to H_0 and K in this way, it follows that Z satisfies the following simple one-dimensional wave equation (the Zerilli equation):

$$\frac{d^2Z}{dr^{*2}}=[V_Z(r^*)-\omega^2]Z. \tag{A35}$$

The effective potential $V_Z(r^*)$ is defined by

$$V_Z(r^*)=\frac{(1-2M/r)}{r^3(nr+3M)^2}[2n^2(n+1)r^3+6n^2Mr^2+18nM^2r+18M^3]. \tag{A36}$$

There exist two linearly independent solutions to this equation. Asymptotically these solutions may be expressed as power series:

$$Z_-(r^*)=e^{-i\omega r^*}\sum_{j=0}^{\infty}\alpha_jr^{-j}, \tag{A37}$$

$$Z_+(r^*)=e^{i\omega r}\sum_{j=0}^{\infty}\bar{\alpha}_jr^{-j}. \tag{A38}$$

The solution Z_- represents purely outgoing gravitational radiation, while Z_+ represents purely ingoing waves. The constants α_j (and their complex conjugates $\bar{\alpha}_j$) may be determined from the recursion relations derived by Chandrasekhar and Detweiler (1975). The relevant coefficients for our purposes here are given by

$$\alpha_1=-i(n+1)\omega^{-1}\alpha_0, \tag{A39}$$

$$\alpha_2=-\tfrac{1}{2}\omega^{-2}[n(n+1)-\tfrac{3}{2}iM\omega(1+2/n)]\alpha_0. \tag{A40}$$

An arbitrary solution to the Zerilli equation will be given by a constant linear combination of Z_+ and Z_-.

Given a specific frequency ω, we have seen that a unique physical solution to the perturbation equations exists in the interior of the stellar model. The boundary values of $H_0(R)$ and $K(R)$ at the surface of the star can be used to determine the boundary values of $Z(R^*)$ and $dZ(R^*)/dr^*$ by using equation (A27). Then $Z(r^*)$ can be determined in the exterior of the star by integrating equation (A35) numerically with these boundary values. In practice we integrate Z from the surface of the star $r=R$, out to a radius $r=25\ \omega^{-1}$. We use a predictor-corrector-modifier integration algorithm with a radial stepsize of $0.05\ \omega^{-1}$. At the point, $r=25\omega^{-1}$, the values of Z and dZ/dr are used to match onto the asymptotic series in equations (A37) and (A38). We keep terms through r^{-2} in these series expansions. The error involved in neglecting the higher terms is expected to be of the order $(r\omega)^3\approx 6\times10^{-5}$ for our computations. By

means of this matching process, we can determine the values of the constants $\beta(\omega)$ and $\gamma(\omega)$,

$$Z(r^*) = \beta(\omega) Z_-(r^*) + \gamma(\omega) Z_+(r^*), \tag{A41}$$

which determine the amount of outgoing and incoming gravitational radiation contained in our solution.

IV. LOCATING THE COMPLEX EIGENFREQUENCIES

The frequencies with which a neutron star naturally oscillates, without being driven by incoming gravitational radiation, are called the eigenfrequencies of the quasi-normal modes. These frequencies will in general be complex, thereby representing the damping of the modes by gravitational radiation emission. The mathematical decomposition of the gravitational field into incoming and outgoing modes was accomplished in equation (A41). To locate those frequencies corresponding to purely outgoing radiation, we must find the roots of the equation

$$\gamma(\omega) = 0. \tag{A42}$$

When $\gamma(\omega)$ vanishes, the metric perturbation will be composed entirely of $Z_-(r^*)$, the outgoing radiation mode, while being devoid of $Z_+(r^*)$, the incoming radiation mode. This then is the mathematical representation of the physically realistic boundary condition which must be specified to determine this eigenvalue problem. We solve this equation by first determining γ numerically for several real values of ω (which are chosen to be as close as possible to the expected eigenfrequency); second, we fit a polynomial in ω to the computed values of γ

$$\gamma(\omega) \approx \gamma_0 + \gamma_1\omega + \gamma_2\omega^2; \tag{A43}$$

third, we determine an approximate root for equation (A42) by locating the roots of the polynomial expansion (A43); and, fourth, we iterate this procedure, using the real part of our approximate root to calculate a new value of γ. We continue this iteration procedure until the real part of the approximate root changes from one step to the next by only about one part in 10^8. This usually requires computing γ for six to eight different frequencies.

In our numerical calculations we take advantage of the fact that the resonance frequencies of neutron stars lie very near the real axis. The imaginary part of the frequency is typically less than 1/1000 of the real part. The smallness of the imaginary part of ω accounts for the difficulties encountered by Thorne (1969*a*, *b*) and Detweiler (1975) in their computations of these frequencies. The smallness of $\mathrm{Im}(\omega)$ allows us to adequately probe the behavior of the function $\gamma(\omega)$ near an eigenfrequency, simply by evaluating it for purely real frequencies near the eigenfrequency. When the frequency ω is real, all of the differential equations for the perturbation functions become purely real also. Therefore, the numerical integrations can be performed with real variables resulting in savings of time and storage space in the computer.

We estimated the accuracy of our numerical computations by increasing the step size in our calculations by a factor of 2 (i.e., we reduce the number of grid points by one-half). We find that the real part of the frequency changes by $\sim \mathrm{Re}\,\Delta\omega/\mathrm{Re}\,\omega \approx 3\times10^{-6}$, while the imaginary part of the frequency changes by $\mathrm{Im}\,\Delta\omega/\mathrm{Im}\,\omega \approx 3\times10^{-5}$. Thus, we feel confident that our eigenfrequencies are accurate to this level. We can also compare the frequencies which we computed for the Harrison-Wheeler equation of state models (model H) with those computed by Thorne (1969*a*, *b*). The real parts of our frequencies agree with Thorne's to about one part in 1000. The imaginary parts of our frequencies agree only at the 40% level, however.

APPENDIX B

PERTURBATION FUNCTIONS NEAR $r = 0$

In this appendix we will obtain the finite solutions to the radial perturbation equations (A21) as a power series about $r = 0$. Therefore we seek a solution of the form:

$$\boldsymbol{Y}(r) = \boldsymbol{Y}(0) + \boldsymbol{Y}'(0)r + \tfrac{1}{2}\boldsymbol{Y}''(0)r^2, \tag{B1}$$

where $\boldsymbol{Y}(0)$, $\boldsymbol{Y}'(0)$, and $\boldsymbol{Y}''(0)$ are constants. These constants are determined by expanding the equations (A21) in a power series about $r = 0$ and solving the equations term by term. The lowest order constants $\boldsymbol{Y}(0)$ have been

determined previously by Thorne and Campolattaro (1967). These constants must satisfy the relationships:

$$H_0(0) = K(0), \tag{B2}$$

$$X(0) = (\rho_0 + p_0)e^{\nu_0/2}\left[\frac{4\pi}{3}(\rho_0 + 3p_0)W(0) - \omega^2 l^{-1}e^{-\nu_0}W(0) + \tfrac{1}{2}K(0)\right]. \tag{B3}$$

(The constants ρ_0, p_0, and ν_0 are defined in equations [B5]–[B7] below.) These equations demonstrate that only two linearly independent bounded solutions exist at $r = 0$. The next order terms in the expansion of the Einstein equations yield the conditions:

$$Y'(0) = 0. \tag{B4}$$

In order to evaluate the next order terms, $Y''(0)$, it will be necessary to evaluate the equilibrium stellar model in a power series expansion also. Thus, we let

$$p(r) = p_0 + \tfrac{1}{2}p_2 r^2 + \tfrac{1}{4}p_4 r^4, \tag{B5}$$

$$\rho(r) = \rho_0 + \tfrac{1}{2}\rho_2 r^2, \tag{B6}$$

$$\nu(r) = \nu_0 + \tfrac{1}{2}\nu_2 r^2 + \tfrac{1}{4}\nu_4 r^4. \tag{B7}$$

The constants p_2, p_4, etc., are evaluated from the series expansion of equations (A3)–(A5):

$$p_2 = -\frac{4\pi}{3}(\rho_0 + p_0)(\rho_0 + 3p_0), \tag{B8}$$

$$\rho_2 = p_2(\rho_0 + p_0)/\gamma_0 p_0, \tag{B9}$$

$$\nu_2 = \frac{8\pi}{3}(\rho_0 + 3p_0), \tag{B10}$$

$$p_4 = -\frac{2\pi}{5}(\rho_0 + p_0)(\rho_2 + 5p_2) - \frac{2\pi}{3}(\rho_2 + p_2)(\rho_0 + 3p_0) - \frac{32\pi^2}{9}\rho_0(\rho_0 + p_0)(\rho_0 + 3p_0), \tag{B11}$$

$$\nu_4 = \frac{4\pi}{5}(\rho_2 + 5p_2) + \frac{64\pi^2}{9}\rho_0(\rho_0 + 3p_0). \tag{B12}$$

We can now evaluate the next term in the expansion of the Einstein equations. We find that the following relationships must hold:

$$\tfrac{1}{2}(l+2)[H_0''(0) - K''(0)] = -\frac{8\pi}{3}(\rho_0 + 3p_0)K(0) - \frac{2\omega^2}{l(l+1)}e^{-\nu_0}[lK(0) + 8\pi(\rho_0 + p_0)W(0)], \tag{B13}$$

$$\begin{aligned}\tfrac{1}{4}(\rho_0 + p_0)H''(0) - \tfrac{1}{2}p_2 W''(0) - \tfrac{1}{2}\omega^2(\rho_0 + p_0)e^{-\nu_0}\frac{l+3}{l(l+1)}W''(0) - \tfrac{1}{2}e^{-\nu_0/2}X''(0)\\ = \tfrac{1}{2}l^{-1}\omega^2 e^{-\nu_0}[\rho_2 + p_2 - \nu_2(\rho_0 + p_0)]W(0) + p_4 W(0) - \tfrac{1}{4}\nu_2 e^{-\nu_0/2}X(0)\\ - \frac{4\pi}{3}\rho_0 p_2 W(0) - \tfrac{1}{4}(\rho_2 + p_2)K(0) - \tfrac{1}{2}\omega^2(\rho_0 + p_0)e^{-\nu_0}F,\end{aligned} \tag{B14}$$

$$\tfrac{1}{2}[l+3+\tfrac{1}{2}l(l+1)]H''(0)-\tfrac{1}{2}[3(l+2)+(l+1)(l+2)+1-\tfrac{1}{2}l(l+1)]K''(0)$$
$$=-\frac{8\pi}{3}\rho_0 l(l+2)K(0)-4\pi(\rho_0+3p_0)K(0)+8\pi\rho-\frac{32\pi^2}{3}\rho_0(\rho_0+p(l+1)W(0)+4\pi l(l+1)(\rho_0+p_0)F, \tag{B15}$$

$$\tfrac{1}{4}(l+2)H''(0)-\tfrac{1}{2}(l+2)K''(0)+\tfrac{1}{2}\omega^2 e^{-\nu_0}W''(0)-\tfrac{1}{4}(l+2)\nu_2 W''(0)+\tfrac{1}{2}(l+2)(\rho_0+p_0)^{-1}e^{-\nu_0/2}X''(0)$$
$$=-\frac{2\pi}{3}\rho_0\nu_2 W(0)+\tfrac{1}{2}(l+2)\nu_4 W_0+\tfrac{1}{2}\omega^2 e^{-\nu_0}\left[\nu_2-\frac{8\pi}{3}\rho_0\right]W(0)-\tfrac{1}{2}\nu_2 K(0)$$
$$+\tfrac{1}{4}l(\rho_0+p_0)^{-1}e^{-\nu_0/2}\left[\nu_2+2(\rho_2+p_2)(\rho_0+p_0)^{-1}\right]X(0)-\tfrac{1}{4}l(l+1)\nu_2 F, \tag{B16}$$

where F is defined by the relationship:

$$F=\frac{2}{l(l+1)}\left[\gamma_0^{-1}p_0^{-1}e^{-\nu_0/2}X(0)+\frac{4\pi}{3}\rho_0(l+1)W(0)+\tfrac{3}{2}K(0)\right]. \tag{B17}$$

These equations (B13)–(B16) have the form

$$\mathbf{T}\cdot\boldsymbol{Y}''(0)=\mathbf{U}\cdot\boldsymbol{Y}(0), \tag{B18}$$

where the matrices $\mathbf{T}$ and $\mathbf{U}$ depend only on l, ω, and the constants which determine the equilibrium stellar model at $r=0$. Therefore, it is a straightforward numerical problem to evaluate $\mathbf{T}$ and $\mathbf{U}$ for a given stellar model. One can then compute the constants $\boldsymbol{Y}''(0)$ simply by inverting the matrix $\mathbf{T}$:

$$\boldsymbol{Y}''(0)=\mathbf{T}^{-1}\cdot\mathbf{U}\cdot\boldsymbol{Y}(0). \tag{B19}$$

These constants allow us to approximate the two linearly independent solutions to equations (A21), $\boldsymbol{Y}_4$ and $\boldsymbol{Y}_5$, which are finite at $r=0$ by using equation (B1).

REFERENCES

Arnett, W. D., and Bowers, R. L. 1974, *Pub. Astr. Univ. Texas*, No. 9, p. 1.
_____. 1977, *Ap. J. Suppl.*, **33**, 415–436.
Arponen, J. 1972, *Nucl. Phys.*, **A191**, 257.
Baym, G., Pethick, C., and Sutherland, P. 1971, *Ap. J.*, **170**, 299.
Bethe, H. A., and Johnson, M. 1974, *Nucl. Phys.*, **A230**, 1.
Boriakoff, V. 1976, *Ap. J. (Letters)*, **208**, L43.
Bowers, R. L., Gleeson, A. M., and Pedigo, R. D. 1975, *Phys. Rev.*, **D12**, 3043.
Campolattaro, A., and Thorne, K. S. 1970, *Ap. J.*, **159**, 847.
Canuto, V., and Chitre, S. M. 1974, *Phys. Rev.*, **D9**, 1587.
Chandrasekhar, S., and Detweiler, S. 1975, *Proc. Roy. Soc. London*, *A*, **344**, 441.
Cline, T. L., *et al.* 1980, *Ap. J. (Letters)*, **237**, L1.
Cohen, J. M., Langer, W. D., Rosen, L. C., and Cameron, A. G. W. 1970, *Ap. Space Sci.*, **6**, 228.
Cordes, J. M. 1976, *Ap. J.*, **208**, 944.
Cordes, J. M., and Hankins, T. H. 1977, *Ap. J.*, **218**, 484.
Detweiler, S. 1975, *Ap. J.*, **197**, 203.
_____. 1980, *Ap. J.*, **239**, 292.
Detweiler, S. L., and Ipser, J. R. 1973, *Ap. J.*, **185**, 685.
Evans, W. D., *et al.* 1980, *Ap. J. (Letters)*, **237**, L7.
Fackerell, E. D. 1971, *Ap. J.*, **166**, 197.
Glass, E. N., and Lindblom, L. 1982, preprint.
Hankins, T. H., and Boriakoff, B. 1978, *Nature*, **276**, 45.
Hartle, J. B., and Thorne, K. S. 1968, *Ap. J.*, **153**, 807.
Ipser, J. R., and Thorne, K. S. 1973, *Ap. J.*, **181**, 181.
Lambert, J. D. 1973, *Computation Methods in Ordinary Differential Equations* (New York: Wiley).
Liang, E. P. T. 1981, *Nature*, **292**, 319.
Mazets, E. P., Golenetskii, S. V., Aptekar, R. L., Guryan, Yu. A., and Il'inskii, V. N. 1981, *Nature*, **290**, 378.
Meltzer, D. W., and Thorne, K. S. 1966, *Ap. J.*, **145**, 514.
Moszkowski, S. 1974, *Phys. Rev.*, **D9**, 1613.
Oda, M. 1981, in *X-Ray Astronomy with the Einstein Satellite*, ed. R. Giaconni (Dordrecht: Reidel), p. 61.
Pandharipande, V. 1971, *Nucl. Phys.*, **A178**, 123.
Pandharipande, V., Pines, D., and Smith, R. A. 1976, *Ap. J.*, **208**, 550.
Price, R., and Thorne, K. S. 1969, *Ap. J.*, **155**, 163.
Ralston, A. 1962, *Math. Comp.* **16**, 431; **17**, 488 (1963).
Ramaty, R., Bonazzola, S., Cline, T. L., Kazanas, D., and Meszaros, P. 1980, *Nature*, **287**, 122.
Ramaty, R., and Lingenfelter, R. E. 1981, *Phil. Trans. Roy. Soc. London*, *A*, **301**, 671.
Ramaty, R., and Meszaros, P. 1981, *Ap. J.*, **250**, 384.
Soglasnov, V. A., Smirnova, T. V., Popov, M. V., and Kuz'min, A. D. 1981, *Astr. Zh.*, **58**, 771.
Serot, B. D. 1979, *Phys. Letters*, **86B**, 146; **87B**, 403 (1979).
Thorne, K. S. 1969*a*, *Ap. J.*, **158**, 1.
_____. 1969*b*, *Ap. J.*, **158**, 997.
Thorne, K. S., and Campolattaro, A. 1967, *Ap. J.*, **149**, 591; **152**, 673 (1967).
Van Horn, H. M. 1980, *Ap. J.*, **236**, 899.
Walecka, J. D. 1974, *Ann. Phys.*, **83**, 491.
Weisskopf, M. C., Elsner, R. F., Sutherland, P. G., and Grindlay, J. E. 1981, *Ap. Letters*, **22**, 49.
Zerilli, F. J. 1970, *Phys. Rev. Letters*, **24**, 737.

LEE LINDBLOM: Enrico Fermi Institute, University of Chicago, 5630 S. Ellis Ave., Chicago, Il 60637

STEVEN L. DETWEILER: Department of Physics, University of Florida, Gainesville, FL 32611